Available online at www.sciencedirect.com
ScienceDirect
Journal of Pharmaceutical and Biomedical Analysis 44 (2007) 110–117
JOURNAL OF PHARMACEUTICAL AND BIOMEDICAL ANALYSIS
www.elsevier.com/locate/jpba

UV–vis and FTIR–ATR spectroscopic techniques to study the inclusion complexes of genistein with β-cyclodextrins

V. Crupi [a], R. Ficarra [b,*], M. Guardo [b], D. Majolino [a], R. Stancanelli [b], V. Venuti [a]

[a] *Dipartimento di Fisica, Facoltà di Scienze MM.FF.NN., Università di Messina, C.da Papardo, S.ta Sperone 31, P.O. Box 55, 98166 S. Agata, Messina, Italy*
[b] *Dipartimento Farmaco-Chimico, Facoltà di Farmacia, Università di Messina, Viale Annunziata, 98168 Messina, Italy*

Received 13 October 2006; received in revised form 29 January 2007; accepted 31 January 2007
Available online 13 February 2007

Abstract

The effect of β-cyclodextrin (β-CyD), (2-hydroxypropyl)-β-cyclodextrin (HP-β-CyD) and methyl-β-cyclodextrin (Me-β-CyD) complexation on the UV absorption of genistein (Gen) was studied in pure water. A phase solubility study was performed, according to the method reported by Higuchi and Connors, to evaluate the changes of isoflavone in the complexation state and the obtained diagrams suggested that it forms complexes with a stoichiometry of 1:1. Then, the solid complexes of genistein with these macrocycles in 1:1 molar ratio were prepared by the co-precipitation method and characterized by FTIR absorption spectroscopy in ATR geometry. The host–guest interactions have been evidenced by monitoring, in the FTIR–ATR spectra, the changes in some guest molecule bands relative to those observed in the spectra of the 1:1 physical mixtures and complexes.

In particular, for the high-frequency O–H stretching band, a quantitative vibrational assignment of the observed sub-bands has been made.

From the results, the inclusion phenomena have been discussed.

Keywords: Genistein; β-Cyclodextrins; Inclusion complexes; UV–vis spectroscopy; Phase-solubility measurements; FTIR–ATR spectroscopy

1. Introduction

β-Cyclodextrins (β-CyDs) are cyclic oligomers connecting seven glucose units via α-(1,4)-linkages, having a toroidal shape with a non-polar inside and two hydrophilic rims. Thanks to their unusual structure, β-CyDs act as molecular hosts for a large variety of guest molecules, polar and non-polar ones, through non-covalent interactions [1]. In order to increase their host qualities, synthetically modified and relatively safe β-CyDs are usually used in parenteral formulations, such as HP-β-CyD and Me-β-CyD [2]. The detailed analysis of the solid inclusion complexes, providing their three-dimensional structure and lattice, can give more information about the interaction force responsible of their formation. Inclusion complexes are now widely used in pharmaceutical industry, for improving the solubility, stability and bioavailability of the guest molecules [3–7], and in other areas such as the food and cosmetic industries and agrochemistry [8,9].

The inclusion complexes of β-CyDs in aqueous solutions have usually been researched using ultraviolet and visible absorption spectroscopy, fluorimetry, phosphorimetry, NMR spectroscopy, chromatography, etc. [10,11]. In the solid state, the usual physical methods such as single-crystal X-ray diffraction (XRD) and neutron diffraction require crystalline samples [12]. On the other side, the inclusion compounds are routinely obtained as an amorphous powder by freeze-drying, spray-drying or co-precipitation. In these cases, X-ray analysis is not suitable for obtaining structural information, since it is not able to discriminate whether the obtained product is a true inclusion complex or a homogeneous dispersed mixture of the two amorphous components, because of the very broad signals and the diffused diffraction pattern. Recently, many papers have been published on the effects of inclusion process on the guest molecules, as investigated by Raman and Fourier transform infrared (FTIR) spectroscopy [13–20]. Generally speaking, the changes observed in the vibrational spectra of the drug in the complex form, with respect to the pure compound and the physical mixture, are indicative of the formation of a drug/cyclodextrin complex. In particular, when used in Attenuated Total Reflectance (ATR) geometry, FTIR spectroscopy

* Corresponding author. Tel.: +39 090 6766553; fax: +39 090 6766407.
E-mail address: rficarra@pharma.unime.it (R. Ficarra).

0731-7085/$ – see front matter © 2007 Elsevier B.V. All rights reserved.
doi:10.1016/j.jpba.2007.01.054

brings significant advantages to pharmaceutical development compared with the usual technique, linked to the fact that, firstly, no sample preparation is required and, secondly, FTIR–ATR spectra can be obtained in a non-invasive way, i.e. without interference due to the usual dispersion of the sample in KBr or CsI pellets. The absence of sample manipulation guarantees rapidity in the measurement process and high reproducibility of the spectra, making FTIR–ATR technique very adequate also in revealing differences in solid-state forms including hydration state and polymorphic crystal forms, and generally in the identification and characterization of pharmaceuticals [21,22]. We also add that this technique represents an excellent opportunity in studying hydrogen bonding, since it allows one to obtain spectra free from saturation artifacts, so overcoming the difficulties linked, for example, to the strong absorption of the O–H fundamental stretching vibration, here analysed. In spite of this, very little has been reported about the inclusion complexes of CyDs in the solid state using FTIR–ATR spectroscopy.

As guest molecule, Gen (4′,5,7-trihydroxyisoflavone, see Fig. 1), the most abundant isoflavone in soybeans, is of intense interest because its activity is involved in a variety of health protective effects including reducing the risk of cardiovascular disease, lowering rates of prostate, inhibition of the cancerous cell growth, and improving bone health among many other claims [23–27]. Because of its chemical structure, the molecule is poorly soluble in water and its dissolution is slow. This imposes some restraints to its therapeutic applications. A strategy to improve its rate of absorption and to achieve a rapid onset of activity consists of the preparation of inclusion complexes with β-CyDs [28,29].

Lee et al. [30] have evaluated the inclusion efficiency of Gen and other guests in β-CyD and HP-β-CyD in 1 wt.% solutions (∼9 mM). In particular, above 5 mM in the case of β-CyD, non-consideration of the formation of aggregates could invalidate the quantitative analysis. Very recently, Cheng et al. [31] by using a variety of well-established techniques, including thermogravimetry (TG), derivative thermogravimetry (DTG) and differential scanning calorimetry (DSC) indicated that both β-CyD and the host Gen molecule form molar ratio 1:1 complex. In addition, the thermal stability and water solubility of Gen are shown to be significantly improved by complexation.

On this basis, the present study was designed to elucidate the mode of complexation between Gen and β-CyD, HP-β-CyD and Me-β-CyD.

The inclusion complexes of Gen with β-CyD, HP-β-CyD and Me-β-CyD were prepared by mixing and shaking in solution and characterized by UV–vis absorption. Then, the solid inclusion complexes were synthesized by co-precipitating. In addition, the physical mixtures of Gen and β-CyD, HP-β-CyD and Me-β-CyD were also prepared by simple blending. The inclusion complexes and the physical mixtures in the solid state were characterized for the first time by FTIR–ATR spectroscopy.

In particular, in order to clarify the nature of the O–H stretching vibration, a new quantitative analysis of the FTIR–ATR spectra has been performed by using mathematical procedures such as deconvolution and curve fitting.

The obtained results allowed us to elucidate the effect of the inclusion process on the guest molecule.

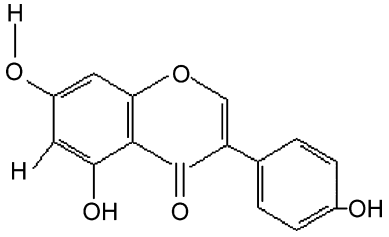

Fig. 1. Chemical structure of genistein (Gen, 4′,5,7-trihydroxyisoflavone).

2. Experimental

2.1. Chemicals

The following reagents and solvents were used: genistein (4′,5,7-trihydroxyisoflavone, $C_{15}H_{10}O_5$, FW 270.24) from Sigma–Aldrich Chemie® (USA); β-cyclodextrin (β-CyD, FW ≈ 1135.0, mp ≈ 290–300 °C dec.), (2-hydroxypropyl)-β-cyclodextrin (HP-β-CyD, FW ≈ 1170.0, mp ≈ 278 °C dec., degree of substitution ≈ 0.6), methyl-β-cyclodextrin (Me-β-CyD, FW ≈ 1310.0, degree of substitution ≈ 1.7–1.9), from Fluka Chemie (Switzerland). They were employed without any further purification. Water used throughout the study was double-distilled and deionised, then filtered trough 0.22 μm Millipore® GSWP filters (Bedford, USA). Solutions to be analyzed were prior filtered trough 0.45 μm Sartorius Minisart®-SRP 15 PTFE filters (Germany).

2.2. UV–vis absorption measurements

UV–vis absorption spectra were obtained with a Perkin-Elmer (Norwalk, USA) UV–vis double beam spectrophotometer mod. Lambda 45 (resolution, $(0.001 \pm 1) \times 10^{-3}$ absorbance units; signal-to-noise ratio, 1×10^{-4}), equipped with a PC for data processing (softwares: UV-Win Lab®, from Perkin-Elmer; Peakfit® v.4.11, from Systat Software Inc.). 10.00 and 1.00 mm pathlength rectangular quartz cells (Hellma) were employed in the 220–400 nm spectral range (scan speed 60 nm/min; slit = 2). Concentrations of the samples to be measured were adjusted so that the extinction values did not exceed $E = 1.0$ at a given wavelength. Baseline was established for each measurement, by placing in the reference compartment an aqueous solution of each cyclodextrin at the same concentration of the sample. All measurements were carried out at 25.0 ± 0.01 °C. All data shown represent the average of, at least, three determinations. UV–vis spectroscopy was employed in the study of Gen alone (10^{-6} M) and in the presence of increasing amounts of macrocycles ($(1.0–9.0) \times 10^{-3}$ M).

2.3. Phase-solubility measurements

Phase-solubility studies were performed with a Telesystem stirring bath thermostat 15.40 with Telemodul 40 C control unit, which allowed an accuracy of 0.01 °C. A fixed amount

of Gen (>10^{-4} M), exceeding its solubility, was added to unbuffered aqueous solutions of β-CyD, HP-β-CyD and Me-β-CyD ((0.0–9.0) × 10^{-3} M) in 10 ml capped tubes, then sonicated in a Bandelin RK 514 water bath (Berlin, Germany) for 15 min. Flasks were sealed to avoid changes due to evaporation and magnetically stirred for 3 days in a thermostated bath at 25.0 ± 0.01 °C, shielded from light to prevent any degradation of the molecules.

After the equilibrium was reached (about 72 h), the suspensions were filtered through Sartorius Minisart®-SRP 15 PTFE 0.20 m filters. An aliquot from each vial was withdrawn by 1 ml glass syringe (Poulten & Graf GmbH, Germany) and assayed spectrophotometrically to evaluate the amount of Gen dissolved. Experiments were carried out in triplicate, solubility data were averaged and used to calculate the binding constant for the complexes formation, by UV–vis absorption spectroscopy.

2.4. FTIR–ATR absorption measurements

FTIR–ATR spectra were recorded, at room temperature (25 ± 0.01 °C), using a Bomem DA8 Fourier transform spectrometer, operating with a Globar source, in combination with a KBr beamsplitter, a DTGS/KBr detector. The powders were contained in Golden Gate diamond ATR system, just based on the Attenuated Total Reflectance (ATR) technique [32]. As well known, when infrared radiation, under certain conditions, passes through a prism made of a high refractive index infrared transmitting material (ATR crystal), it will be totally reflected. In a ATR measurement, the sample (powder) is placed in contact with the totally reflecting surface of the ATR crystal and pressed by a diamond piston. In this configuration, a wavelength range from 600 to 4000 cm^{-1} can be covered. In this way a well-defined layer of sample is obtained. In this configuration, the evanescent wave will be attenuated in regions of the IR spectrum where the sample absorbs energy. A property of the evanescent wave that makes ATR a powerful technique is that the intensity of the wave decays exponentially with a distance from the surface of the ATR crystal. The distance, on the order of micrometers, makes ATR generally insensitive to sample thickness, allowing for the analysis of thick or strongly absorbing samples. The spectra were recorded with a resolution of 2 cm^{-1}, automatically adding 100 repetitive scans in order to obtain a good signal-to-noise ratio and highly reproducible spectra. All the IR spectra were normalized for taking into account the effective number of absorbers.

No smoothing was done, and spectroscopic manipulation such as baseline adjustment and normalization were performed using the Spectracalc software package GRAMS (Galactic Industries, Salem, NH, USA). The band decomposition of the O–H stretching mode was undertaken using the curve fitting routine provided in the PeakFit 4.0 software package, which enabled the type of fitting function to be selected. The strategy adopted was to use well-defined shape components of Voigt functions with all the parameters allowed to vary upon iteration. The statistical parameters were used as a guide to "best-fit".

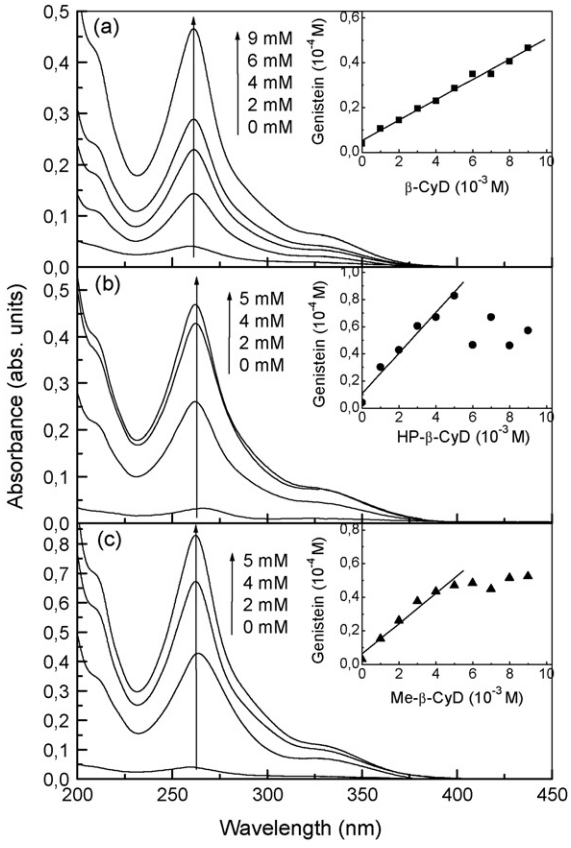

Fig. 2. UV absorption spectra of Gen in the presence of increasing concentrations of: (a) β-CyD (0.0–9.0 mM), (b) HP-β-CyD (0.0–5.0 mM), and (c) Me-β-CyD (0.0–5.0 mM). In the corresponding insets, phase solubility diagrams of Gen as a function β-CyD, HP-β-CyD, and Me-β-CyD concentration in water at 25.0 ± 0.1 °C are shown.

3. Results and discussion

3.1. Phase-solubility studies

The stoichiometric ratios and stability constants describing the extent of formation of the complexes were obtained by measuring the changes in UV–vis absorbance of the substrates, in the presence of increasing concentrations of the ligands. As you can see in Fig. 2(a)–(c), the absorption intensities increased by increasing the β-CyD, HP-β-CyD and Me-β-CyD concentration. In the same figure, the insets show the phase-solubility diagrams obtained for Gen with β-CyD, HP-β-CyD and Me-β-CyD, respectively. As it appears clear from an inspection of the figure, for all the drug/CyD systems the solubility of the Gen is enhanced by the presence of the macrocycle.

In particular, a linear increase in solubility of Gen with concentration of β-CyD is observed in all the explored range, whereas there is a negative shift from linearity with a well defined plateau at 5 × 10^{-3} M for HP-β-CyD and Me-β-CyD; indicating that at this point Gen must be fully complexed.

In the region where a linear increase was observed, a linear regression analysis was performed and the equations turned out to be as follows:

$$y = 0.0454x + 0.0528 \quad (1)$$

for Gen/β-CyD system:

$$y = 0.1493x + 0.1065 \quad (2)$$

for Gen/HP-β-CyD system, and, finally:

$$y = 0.0899x + 0.0628 \quad (3)$$

for Gen/Me-β-CyD system. In the above expressions, x is the concentration of cyclodextrin in solution (10^{-3} M); y is the concentration of Gen in solution (10^{-4} M); the correlation coefficient turned out to be $r^2 = 0.97$ in all cases.

Since the slope of the diagram is less than 1, the soichiometry of the complexes was assumed to be 1:1. Then, the stability constants, K_c, were calculated from the straight-line portion of the phase-solubility diagram [33], according to the following equation:

$$K_c = \frac{\alpha}{S_0(1-\alpha)} \quad (4)$$

where α is the slope of the linear plot reporting the amount of complexed Gen as a function of CyDs and $S_0 = 2.9 \times 10^{-6}$ M is the solubility of isoflavone in water, as experimentally obtained by distributing the guest molecule between water and butanol after having already calculated the extinction molar coefficient (ε) of Gen in this organic solvent [34].

A smaller K_c value indicates too weak an interaction, whereas a larger value indicates the possibility of limited release of drug from the complex thereby interfering with drug absorption. In particular, the highest value for the stability constant was calculated for the complex with HP-β-CyD ($K_c = 60518\ M^{-1}$), and then, in order, for Me-β-CyD ($K_c = 34065\ M^{-1}$) and β-CyD ($K_c = 16401\ M^{-1}$).

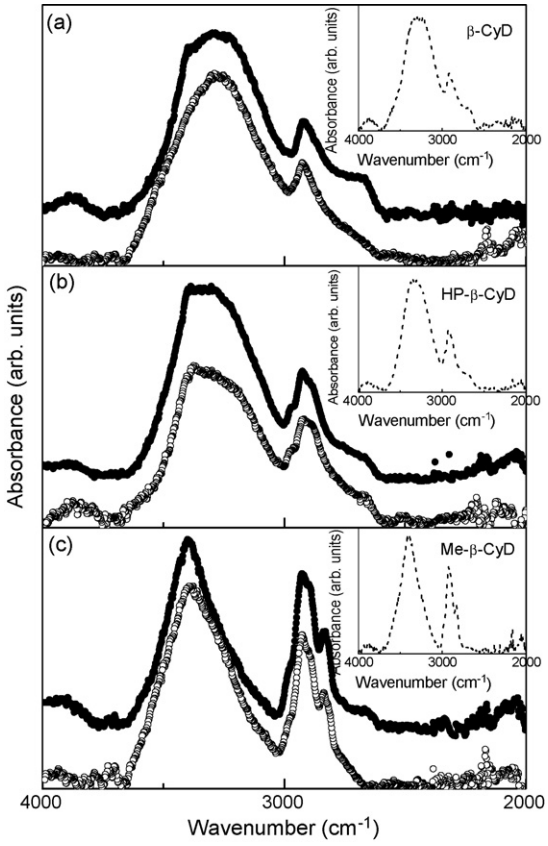

Fig. 3. FTIR–ATR spectrum in the 4000–2000 cm^{-1} region of (a) Gen/β-CyD, (b) Gen/HP-β-CyD, and (c) Gen/Me-β-CyD systems. Closed circles refer to physical mixtures and open circles refer to inclusion complexes. In the insets, the FTIR–ATR spectra of the corresponding pure macrocycles are reported.

3.2. FTIR–ATR absorption measurements

The inclusion complexes of Gen with β-CyD, HP-β-CyD and Me-β-CyD were obtained by co-precipitation method.

A fixed amount of Gen was weighted and dissolved in purified water and an equimolar concentration of each macrocycle was added to obtain the complexes in a molar ratio 1:1.

Stirring was carried out for one hour, under controlled temperature (25 ± 0.01 °C). After that time, solutions were stored in the dark at 4 °C for about 24 h and the water was subsequently evaporated under vacuum (∼30 °C), obtaining the Gen/β-CyD, Gen/HP-β-CyD, Gen/Me-β-CyD solid complexes.

The infrared spectra of the Gen/β-CyD, Gen/HP-β-CyD, and Gen/Me-β-CyD complexes were analysed and compared with the spectra of the pure compounds and their physical mixtures, respectively.

In the high frequency region, we focused our attention on the 4000–2000 cm^{-1} range. As it is known, the infrared spectrum of Gen presents, in this range, a band at ∼3405 cm^{-1} typical of the vibrational frequency of the O–H stretching mode, overlapped with another broad band, peaked at ∼3084 cm^{-1}, assigned to C–H stretching vibration [35].

In the case of Gen/β-CyDs physical mixtures and complexes, the O–H stretching vibrational modes coming from primary and secondary O–H groups of β-CyDs, from crystallization water molecules (interstitial and intracavity), and from the hydroxyl groups of the guest molecules are revealed in the ∼3700 to ∼3100 cm^{-1} range [36,37]. In principle, these contributions, that usually appear overlapped, give rise to very broad bands, and this makes the analysis of this spectral profile not easy. The C–H stretching contribution is also evident at ∼2930 cm^{-1}. In a general way, we can adfirm that the effect of the guest molecules on the position and intensities of these bands depends on both the size and the rearrangement of the guest within the host cavity. As reported in Fig. 3, the O–H stretching experimental spectra of Gen/β-CyD, Gen/HP-β-CyD, and Gen/Me-β-CyD complexes exhibit a different profile with respect to the ones corresponding to the physical mixtures. This occurrence could suggest a redistribution, upon complexation, of the water molecules among the different hydrogen bonds sites, because of the formation of hydrogen bond between Gen and β-CyDs. Probably, during the complexation process, Gen enters into the β-CyDs torus-shaped cavity, disturbing some of the previous existing bonds formed between the O–H groups of β-CyDs molecules, and the water molecules from the inside of the torus change their hydrogen bonding environment. In particular, a more enhanced low-frequency contribution together with an overall broadening of the band shape are revealed in the spectra of the complexes with respect to the corresponding physical mixtures, indicating that the observed change in the hydrogen bonding scheme,

as a consequence of complexation, should imply an increased co-operativity involving longer lifetimes.

A quantitative analysis of the observed profiles, including deconvolution and curve-fitting, is then really helpful in order to clarify the nature of the O–H stretching band.

A problem which arises in the analysis of our spectra is the partial overlapping of the C–H and O–H stretching bands. In order to separate both bands and at the same time to resolve the O–H stretching band into components, we choose to fit simultaneously the whole spectrum (C–H and O–H stretching regions) into Voigt components (three for C–H band and five for O–H band), with all the fitting parameters left free to vary upon iteration until converging solution is reached. Then, the contributions coming from the symmetric and antisymmetric methyl stretches have been subtracted from the total fits and more detailed fits have been performed just in the O–H stretching region. Again, five components for the O–H stretching band describe correctly the existing types of H-bonded OH oscillators for all the analysed samples. The results from the curve fitting procedure obtained in the case of β-CyD, HP-β-CyD, and Me-β-CyD are displayed in Fig. 4 and reported in Table 1.

Although the spectral decompostion procedures have no unique solution, we remark that the one we adopted here uses the minimum number of parameters and, at the same time, it furnishes extremely good fits to the data. The best-fit is, in fact, characterized by r^2 ~0.9999 for all the investigated systems. Furthermore, we will show below that it provides a sound tool to quantitatively account for the changes in H-bond scheme upon complexation. On the other side, the presence, in the experimental spectra, of five sub-bands with the assigned centre-frequencies was also suggested by the analysis of the second derivative profiles that showed five minima approximately corresponding to the maxima of each band component. As an example, the case of HP-β-CyD is reported in the inset of Fig. 4(b).

The frequencies we got in fitting our data appeared very similar to those obtained by Gavira et al. [36], then the assignment of the components was performed in agreement with their study. In particular, the sub-band ω_1 at ~3580 cm^{-1} was ascribed to the cluster of water molecules inside the hydrophobic β-CyD cavity. The bands ω_3 ~3410 cm^{-1} and ω_5 ~3174 cm^{-1} were mainly associated to water molecules in the interstices among different β-CyD molecules and linked to them *via* hydrogen bond, even if they also reflect contributions coming from primary and secondary OH groups. These OH groups are, on the other side, responsible of the components revealed at ω_2 ~3525 cm^{-1} and ω_4 ~3280 cm^{-1}. Fig. 5 shows the fitting results obtained for Gen/Me-β-CyD physical mixture and complex, as an example. Table 2 shows the main fitting parameters of the resolved components, i.e. peak wavenumber and relative intensity, for all the investigated Gen/β-CyDs physical mixtures and complexes.

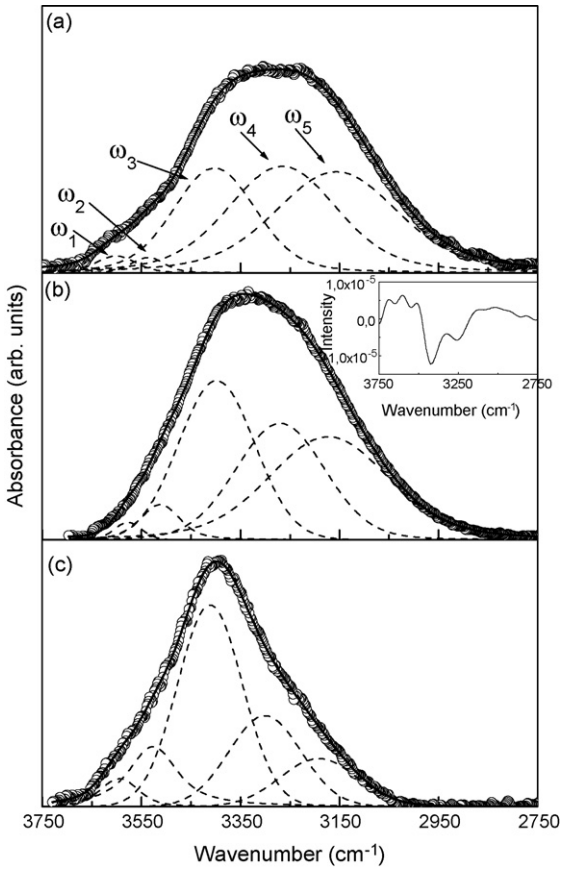

Fig. 4. FTIR–ATR spectrum (open circles) in the 3750–2750 cm^{-1} region of: (a) β-CyD, (b) HP-β-CyD, (c) Me-β-CyD, together with the best-fit (continuous line) and the deconvolution components (dashed lines). In the inset of (b), the second derivative profile of the FTIR–ATR spectrum of HP-β-CyD is also reported.

For each sample, we verified that the physical mixture experimental spectrum turned out to be a complete superposition of the spectra of Gen and the corresponding pure macrocycle. Then, the observed six sub-bands have to reflect the aforementioned contributions coming from β-CyDs, and for this reason they have been labeled again from ω_1 to ω_5, together with the contribution coming from Gen, ω_{Gen}, that, as it is expected, is downshifted in frequency with respect to pure Gen, indicating a more hindered O–H vibration due to the "activation" of some interaction.

The peak wavenumbers are linked to the connectivity of the respective H-bonds: the higher is the connectivity of the arrangement in which the OH oscillator is involved, the more downshifted is the corresponding O–H stretching frequency. Passing from physical mixtures to inclusion complexes, we

Table 1
Best fit parameters of O–H stretching band for all the analysed macrocycles

	ω_1 (cm^{-1})	I_1 (%)	ω_2 (cm^{-1})	I_2 (%)	ω_3 (cm^{-1})	I_3 (%)	ω_4 (cm^{-1})	I_4 (%)	ω_5 (cm^{-1})	I_5 (%)
β-CyD	3581.5	1.9	3536.8	1.5	3422.5	24.8	3265.7	34.6	3156.3	37.2
HP-β-CyD	3576.9	1.2	3511.8	4.2	3398.2	31.3	3269.7	27.9	3172.5	35.4
Me-β-CyD	3594.5	4.2	3526.7	14.2	3411.4	45.1	3300.5	22.9	3192.1	12.9

Table 2
Best fit parameters of O—H strechting band for genistein and for all the analysed physical mixtures (p.m.) and complexes (co.)

	ω_1 (cm^{-1})	I_1 (%)	ω_2 (cm^{-1})	I_2 (%)	ω_3 (cm^{-1})	I_3 (%)	ω_{Gen} (cm^{-1})	I_{Gen} (%)	ω_4 (cm^{-1})	I_4 (%)	ω_5 (cm^{-1})	I_5 (%)
Gen/β-CyD p.m.	3592.0	1.4	3513.6	4.7	3419.8	12.9	3348.2	21.3	3250.8	23.7	3154.9	36.0
Gen/β-CyD co.	3602.8	0.5	3535.9	3.6	3343.3	22.4	3326.9	20.9	3232.1	13.2	3128.5	39.4
Gen/HP-β-CyD p.m.	3588.6	2.4	3475.1	4.0	3403.9	23.5	3334.2	14.6	3255.9	15.1	3159.4	40.2
Gen/HP-β-CyD co.	3610.4	0.6	3515.3	3.6	3384.7	40.6	3306.9	6.3	3219.4	7.2	3147.9	41.6
Gen/Me-β-CyD p.m.	3573.1	3.6	3503.8	8.1	3413.1	38.8	3338.8	15.2	3268.9	15.8	3171.2	18.4
Gen/Me-β-CyD co.	3603.0	0.9	3533.3	7.2	3404.5	44.9	3306.5	9.5	3250.7	10.8	3139.8	26.7

revealed, for all the analysed systems, a total variation of, at most, ∼30 cm^{-1}, and it does not allow us to unequivocally assign a maximum. Anyway an inspection of Table 2 shows, as a general trend, a decreasing of the connectivity of the bonds involved in the highest frequency contributions, ω_1 and ω_2. This means that the corresponding arrangements are less structured. Going down in frequency, passing from ω_3 to ω_5, the opposite behaviour is revealed.

The relative areas of the components are representative of the fractional populations of the particular species present. Passing from physical mixtures from inclusion complexes, for all the analysed systems, we observe, first of all, a decrease of the intensity I_1 of the highest frequency sub-band ω_1. This change indicates a reduction of the number of H_2O molecules included in the cyclodextrins cavities, as a consequence of the entrance, during the inclusion complex process, of Gen inside the cavity. Going on, the decreasing of I_2 and, in particular, of I_4 specifically connected to the stretching of primary and secondary OH groups of β-CyDs, can be justified by thinking that these groups are now involved in different, new, H-bonded schemes, with Gen or other H_2O molecules, indicative of complexation, that contribute to the observed increasing of I_3 and I_5. Finally, we notice that, on one side, ω_{Gen} shows the largest downshift, and, on the other side, I_{Gen} exhibits the most significative decreasing in the case of HP-β-CyD. These occurrences are in agreement with the highest value of K_c here obtained by UV–vis data.

Evidences of the formation of the complexes are clearly present in the spectral region below 1700 cm^{-1}.

In the case of Gen, several intense bands usually appear in this region. These bands would constitute an excellent candidate to show some variation attributable to the complexation process. In particular, the vibrational frequency of C=O stretching is revealed at ∼1649.8 cm^{-1}. Going on, the C=C and the C–O–C stretching vibrational frequencies are observed at ∼1612.4 cm^{-1} and ∼1312–1140 cm^{-1}, respectively [38]. The ∼1260–1030 cm^{-1} range is assigned to the C–O stretching vibration [39].

Figs. 6–8 show the FTIR–ATR spectra of the Gen/β-CyD, Gen/HP-β-CyD, and Gen/Me-β-CyD complexes, respectively,

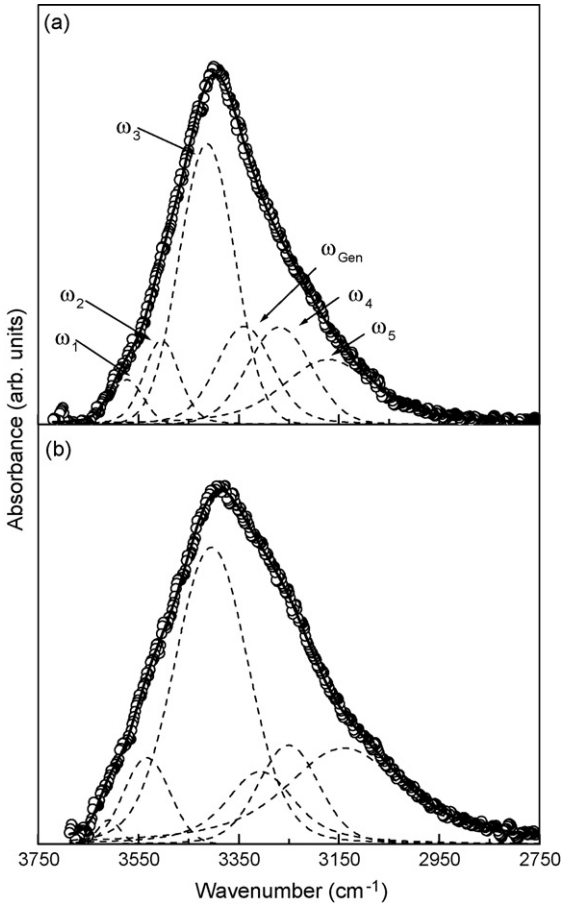

Fig. 5. FTIR–ATR spectrum (open circles) in the 3750–2750 cm^{-1} region of: (a) Gen/Me-β-CyD physical mixture, (b) Gen/Me-β-CyD inclusion complex, together with the best-fit (continuous line) and the deconvolution components (dashed lines).

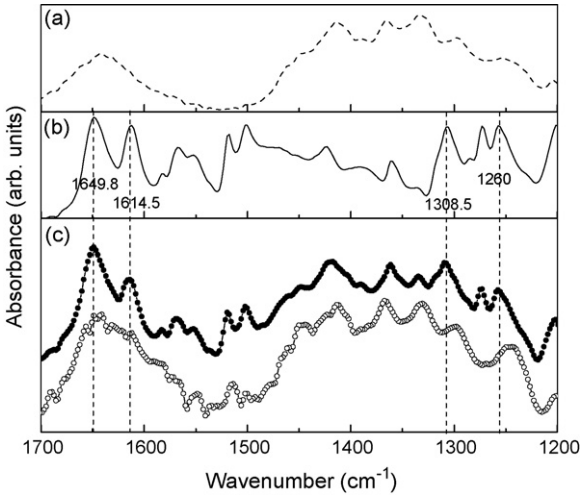

Fig. 6. FTIR–ATR spectrum (1700–1200 cm^{-1} region) of: (a) β-CyD (dashed line), (b) Gen (solid line), (c) Gen/β-CyD physical mixture (closed circles) and Gen/β-CyD complex (open circles).

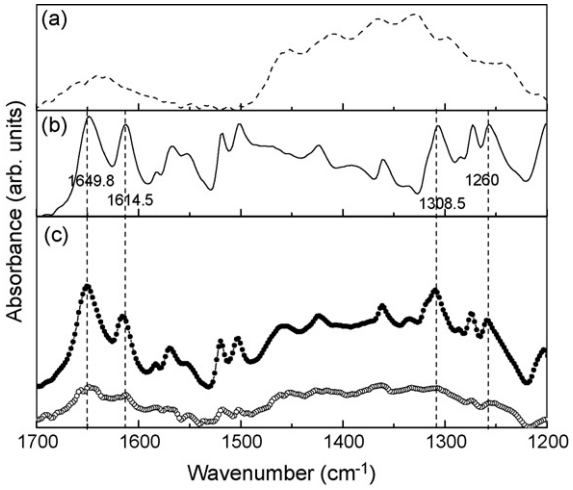

Fig. 7. FTIR–ATR spectrum (1700–1200 cm^{-1} region) of: (a) HP-β-CyD (dashed line), (b) Gen (solid line), (c) Gen/HP-β-CyD physical mixture (closed circles) and Gen/HP-β-CyD complex (open circles).

together with those of the pure compounds and their physical mixture in the 1700–1200 cm^{-1} range. In particular, for all the analysed cases, the C=O stretching (∼1649.8 cm^{-1}), the C=C stretching (∼1614.5 cm^{-1}), the C–O–C stretching (∼1308.5 cm^{-1}), and the C–O stretching (∼1260 cm^{-1}) peaks are also distinctly present, at the same centre-frequencies, in the physical mixtures (although somewhat overlapped by CyDs bands), whereas they appear bumped and diminished in intensity in the spectra of the complexes. In particular, by looking in detail at the 1350–1200 cm^{-1} region, we can distinguish, as far as the C–O–C stretching vibration is concerned, a low-frequency shift in the case of the analysed complexes with respect to the pure Gen and physical mixtures. Similarly, the C–O stretching vibration for all the analysed complexes is shifted to a lower wavenumber than that of pure Gen and physical mixtures. These changes in vibrational frequencies might be ascribed to a weakening of the strength of the interatomic bonds (C–O and C–O–C in our cases) as a consequence of an altered environment around these bonds upon complexation, that induces the formation of new intermolecular hydrogen bonds between Gen and β-CyDs, according to the mechanism already described for explaining the spectral changes revealed in the O–H stretching region.

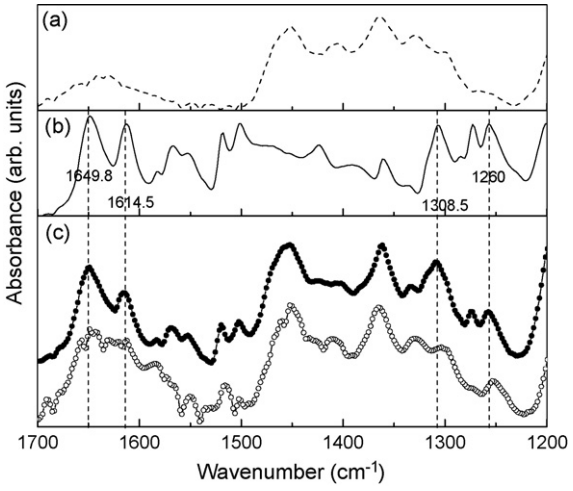

Fig. 8. FTIR–ATR spectrum (1700–1200 cm^{-1} region) of: (a) Me-β-CyD (dashed line), (b) Gen (solid line), (c) Gen/Me-β-CyD physical mixture (closed circles) and Gen/Me-β-CyD complex (open circles).

Finally, a close fitting within the cavity would hinder the out-of-plane bending of aromatic C–H bonds, at ∼790 cm^{-1} in the spectrum of Gen, consequently strongly decreasing the intensity of the vibration mode. This diminishing has been revealed also in the spectra of all our analysed samples, passing from the physical mixtures to the complexes.

All these results allow us to hypothesize that these analysed functional groups are directly involved in the process of complexation with β-CyDs, in a similar basic complexation mechanism for all the analysed host molecules.

4. Conclusions

The effect of β-cyclodextrin, (2-hydroxypropyl)-β-cyclodextrin and methyl-β-cyclodextrin on the UV–vis absorption of genistein has been studied, in pure water.

The effect of cyclodextrins complexation has been observed and, in each case, an increased apparent solubility has been viewed in the medium. This result is of special interest for practical purposes in the pharmaceutical field, since formulations that produce higher drug concentrations in solution may provide improved therapeutic options for patients.

The concentration of the complexed substrates has been obtained from UV–vis intensity values. Thus, after plotting these quantities as a function of the total CyDs concentration, the associated binding constants have been estimated from the slope of the linear fit.

Then, FTIR–ATR spectroscopy has been successfully used to study the complexes formed between β-CyD, HP-β-CyD and Me-β-CyD with Gen in solid phase, in order to investigate host–guest interactions at molecular level. Changes in the FTIR–ATR band-shapes of the complexes compared with their corresponding bands of the pure Gen and physical mixtures have been observed. Differences in the degree of association *via* H-bonding during complexation process have been postulated to explain the spectral changes revealed, at high frequency, in the O–H stretching profile, and, at low frequency, in the C=O, C=C, C–O–C and C–O stretching vibrations. In particular, the analysis of the O–H stretching band by a decomposition into sub-bands appeared very adequate to get quantitative information on the changes induced on the various H-bonded environments during the complexation process. In addition, the disappearing of the out-of-plane bending C–H band of the aromatic moiety suggested a hindering due to a close fit to the cavity.

FTIR–ATR technique has been found a suitable method for the characterization of inclusion phenomena and it appears very promising for the study of other inclusion complexes as well, especially if used in conjunction with other experimental techniques and/or numerical approaches.

References

[1] A.M. Amado, A.M. Moreira da Silva, P.J.A. Ribeiro-Claro, J.J.C. Teixeira-Dias, J. Raman Spectrosc. 31 (2000) 971–978.
[2] V.J. Stella, R.A. Rajewsky, Pharm. Res. 14 (1997) 556–567.
[3] J. Szejtli, Med. Res. Rev. 14 (1994) 353–386.
[4] M.L. Calabrò, S. Tommasini, P. Donato, D. Raneri, R. Stancanelli, P. Ficarra, R. Ficarra, C. Costa, S. Catania, C. Rustichelli, G. Gamberini, J. Pharm. Biomed. Anal. 35 (2004) 365–377.
[5] S. Scalia, A. Casolari, A. Iaconinoto, S. Simeoni, J. Pharm. Biomed. Anal. 30 (2002) 1181–1189.
[6] K.L. Park, K.H. Kim, S.H. Jung, H.M. Lim, C.H. Hong, J.S. Kang, J. Pharm. Biomed. Anal. 27 (2002) 569–576.
[7] J.M. Moreno-Cerezo, M. Cíaz, D. Cíaz, M. Córdoba-Borrego, J. Pharm. Biomed. Anal. 26 (2001) 417–426.
[8] L. Zhang, S. Lerner, W.V. Rustrum, G.A. Hofman, Bioelectrochem. Bioenerg. 48 (1999) 453–461.
[9] Y.L. Loukas, V. Vraka, G. Gregoriadis, Inter. J. Pharm. 117 (1996) 225–231.
[10] M.L. Calabrò, S. Tommasini, P. Donato, R. Stancanelli, D. Raneri, S. Catania, C. Costa, V. Villari, P. Ficarra, R. Ficarra, J. Pharm. Biomed. Anal. 36 (2005) 1019–1027, and references therein.
[11] S. Tommasini, M.L. Calabrò, R. Stancanelli, P. Donato, C. Costa, S. Catania, V. Villari, P. Ficarra, R. Ficarra, J. Pharm. Biomed. Anal. 39 (2005) 572–580, and references therein.
[12] D. Le Bas, N. Rysanek, in: D. Duchêne (Ed.), Cyclodextrins and Their Industrial Uses, Editions de Santé, Paris, 1987, pp. 105–130.
[13] B. Rossi, P. Verrocchio, G. Viliani, G. Scarduelli, G. Guella, I. Mancini, J. Chem. Phys. 125 (2006) (Art. 044511).
[14] T. Iliescu, M. Baia, V. Miclăuş, Eur. J. Pharm. Sci. 22 (2004) 487–495.
[15] A. Bertoluzza, M. Rossi, P. Taddei, E. Redenti, M. Zanol, P. Ventura, J. Mol. Struct. 480–481 (1999) 535–539.
[16] I. Bratu, A. Hernanz, J.M. Gavira, G.H. Bora, Rom. J. Phys. 50 (2005) 1063–1069.
[17] A. Pravin Mukne, M.S. Nagarsenker, AAPS Pharm. Sci. Technol. 5 (2004) (Art. 19).
[18] E. Bilensoy, M. Abdur Rouf, I. Vural, M. Şen, A. Atilla Hincal, AAPS Pharm. Sci. Technol. 7 (2006) (Art. 38).
[19] S.H. Choi, S.Y. Kim, J.J. Ryoo, J.Y. Park, K.P. Lee, Anal. Sci. 17 (2001) 785–788.
[20] S.H. Choi, J.W. Seo, S.I. Nam, M.S. Lee, K.P. Lee, J. Incl. Phenom. Macrocycl. Chem. 40 (2001) 279–283.
[21] F. Lewiner, J.P. Klein, F. Puel, G. Fevotte, Chem. Eng. Sci. 56 (2001) 2059–2084.
[22] B.D. Hahn, R.H.H. Neubert, S. Wartewig, A. Christ, C. Hentzsch, J. Pharm. Sci. 89 (2000) 1106–1113.
[23] J.J. Raffoul, Y. Wang, O. Kucuk, J.D. Forman, F.H. Sarkar, G.G. Hillman, BMC Cancer 6 (2006) (Art. 107).
[24] A. Nedeljković, S. Radulović, S. Bjelogrlić, Arch. Oncol. 9 (2001) 171–174.
[25] Y.Y. Xu, C. Yang, S.N. Li, Life Sci. 79 (2006) 828–837.
[26] K.S. Suh, G. Koh, C.Y. Park, J.T. Woo, S.W. Kim, J.W. Kim, I.K. Park, Y.S. Kim, Phytochemistry 63 (2003) 209–215.
[27] J. Boersma, S. Barnes, M. Kirk, C.C. Wang, M. Smith, H. Kim, J. Xu, R. Patel, V.M. Darley-Usmar, Mutat. Res.-Fund. Mol. M 480–481 (2001) 121–127.
[28] Y.J. Lei, J.X. Shi, F.D. Liu, Chin. Pharm. J. 39 (2004) 837–839.
[29] K. Polkowsky, J.Cz. Dobrowolsky, J. Pachecka, A.P. Mazurek, Acta Pol. Pharm.-Drug Res. 56 (1999) 109–116.
[30] S.H. Cho, S.Y. Kim, S.I. Lee, Y.M. Lee, J. Ind. Eng. Chem. 12 (2006) 50–59.
[31] S. Cheng, L. Du, M. Niu, M. Zhu, Food Sci. 27 (2006) 94–99.
[32] V. Crupi, F. Longo, D. Majolino, V. Venuti, J. Chem. Phys. 123 (2005) (Art. 154702).
[33] T. Higuchi, K.A. Connors, Adv. Anal. Chem. Instrum. 4 (1965) 117–212.
[34] R. Stancanelli, A. Mazzaglia, S. Tommasini, M.L. Calabrò, V. Villari, M. Guardo, P. Ficarra, R. Ficarra, J. Pharm. Biomed. Anal., submitted for publication.
[35] S. Usha, I.M. Johnson, R. Malathi, J. Biochem. Mol. Biol. 38 (2005) 198–205.
[36] J.M. Gavira, A. Hernanz, I. Bratu, Vib. Spectrosc. 32 (2003) 137–146.
[37] I. Bratu, F. Veiga, C. Fernandes, A. Hernanz, J.M. Gavira, Spectroscopy 18 (2004) 459–467.
[38] P.L. Soni, H.M. Chawla, Text Book of Organic Chemistry, Sultan Chand and Sons, New Delhi, 1994, pp. 1257–1279.
[39] R.M. Silvestrin, F.X. Wabster, Spectrometric Identification of Organic Compounds, John Wiley and Sons, New York, 1997, pp. 95–180.